ISSN 1068-798X, Russian Engineering Research, 2015, Vol. 35, No. 7, pp. 517–529. © Allerton Press, Inc., 2015.
Original Russian Text © A.P. Kuznetsov, 2015, published in Vestnik Mashinostroeniya, 2015, No. 4, pp. 76–87.

Structure of Cutting Processes and Equipment. Part 3. Structure of Cutting Processes[1]

A. P. Kuznetsov

Stankin Moscow State Technical University, Moscow
e-mail: stankin-okm@yandex.ru

Abstract—Metal-cutting processes are considered, on the basis of physical models. The parts and equipment used for cutting are analyzed.

Keywords: technological processes, cutting, classification, structure

DOI: 10.3103/S1068798X15070096

The technological construct of the cutting-process structure may be written in the following form, according to the classification (Table 5) and procedure for formation of structural components (Figs. 5–7) in [1]

$$T(7) = [F_f(123456), P_k(123456), P_v(123456)]$$
$$= [F_f(134678), P_k(15253645), P_v(162636)].$$

In what follows, cutting will be regarded as a machining process that, in physical terms, involves the interaction of two solids: the part and the tool. Obviously, other physical processes in which the mass of the part is reduced may be considered analogously, but in that case the interaction is between a solid body and the tool in a different state (hydraulic cutting, gas cutting, plasma cutting, etc.) or a solid body and a physical field (laser cutting, electrophysical methods, etc.).

If the cutting process is regarded as a system, we may analyze the structural elements, whose content, number, and parameter relations characterize the properties of the cutting system [2, 3]. We consider the following structural elements of the cutting system and their relations:

—a physical model;

—a physical process: mechanics (statics, kinetics, dynamics), continuum mechanics (elastic and plastic deformation), solid-state physics (dislocations);

—physical phenomena: mechanical (disintegration), thermal, electromagnetic, or chemical;

—diagrams of the process: elements, parameters, properties;

—structures of the process: elements, constraints, relations;

—description (structural–logical, mathematical, analog) of the structural changes and behavior;

—implementation of the process model: mechanisms, machines, equipment, systems.

Conceptually, the analysis of all aspects of metal cutting is based on the fundamental physical formulation of the problem, with the following principles [2, 3]:

—the physical model involves the removal (or splitting) of material;

—the physical process is deformation (elastic or plastic);

—the physical phenomenon is disintegration on account of the formation of dislocations and cracks.

Note that, according to continuum mechanics, a crack is understood to be a macrocrack, whereas solid-state physics is based on the concept of a microcrack. For any elasticity-theory problem, the stress and displacement fields close to the crack tip are found to be of almost the same structure. That permits the creation of physical models of the splitting of material (displacement of surface layers of the crack), as shown in Fig. 10 [4].

Model I (rupture or normal fracture) corresponds to the displacement of surface layers of the crack, which diverge in opposite directions.

Model II (a transverse-shear crack) corresponds to the displacement of surface layers of the crack, which slip past one another.

Model III (a longitudinal- or antiplane-shear crack) corresponds to the displacement of surface layers of the crack, which slip parallel to the front of the crack.

In dislocation theory, models I–III correspond to wedge, edge, and screw dislocations.

[1] Parts 1 and 2 appeared in the previous two issues. Part 4 will appear in the next issue. The numbering of the tables and figures continues from the previous parts.

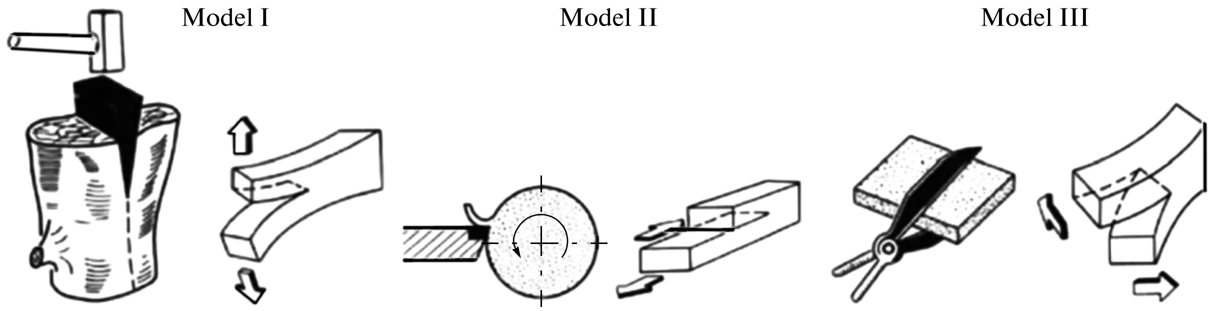

Fig. 10. Physical models of types of crack-surface displacement [4].

For all three models, the equations for the stress and displacement fields are analogous [4, 5]

$$\left.\begin{aligned} \sigma &= (K/\sqrt{2\pi r})f_\sigma(\theta); \\ \tau &= (K/\sqrt{\pi r})f_\tau(\theta); \\ u &= (K/\mu)g_u(\theta)\sqrt{(r/2\pi)}; \\ v &= (K/\mu)g_v(\theta)\sqrt{(r/2\pi)}, \end{aligned}\right\} \quad (1)$$

where $K = K_\text{I}$, K_II, K_III are stress-intensity coefficients depending on the external load and the dimensions of the body, MPa $\text{m}^{1/2}$; r, θ are the radial (m) and angular (deg) coordinates; μ is the Lame elastic constant; $f(\theta)$, $g(\theta)$ are functions that depend only on the angle.

The literature includes tables of analytical expressions for the stress-intensity coefficients corresponding to bodies of different configuration, with different loads. According to Eq. (1), the stress state at the crack tip is described by stress-intensity coefficients. That permits judgments regarding the limiting equilibrium of the crack and its distribution. Accordingly, the onset of crack propagation is the basic criterion of failure mechanics.

Deformation of the machined (split) material on cutting is due to the normal and tangential components of the stress. The plastic deformation of the material under the action of the tangential stress is the relative displacement of volumes of deformed material without loss of integrity. By contrast, failure with rupture of the material is determined by the normal stress. The onset of plastic deformation is observed when the intensity of the tangential stress reaches the shear yield point; the culmination of the process is macrodisintegration, when the damage score for the material is one [6].

Linear failure mechanics describes brittle failure, which occurs as a result of crack enlargement with little or no plastic deformation at the crack tip. If the characteristic linear dimension of the plastic zone at the crack tip is more than 20% greater than the crack length, the behavior of the body with a crack is described by nonlinear failure mechanics, characterizing a relatively developed plastic zone at the crack tip [5]. This indicates that, as plastic deformation develops, its gradient at the crack tip and the shape of the plastic zones will change. The elastoplastic deformation and dimensions of the plastic zones increase with the rated stress, but this relation is not proportional. Hence, to select a physical model, we need to have some idea of the shape and characteristic dimension of the plastic zone, the effective strain, and the change in these parameters with variation in the load. Within a small vicinity of the crack tip, plastic deformation is observed when the stress is small relative to the yield point. With increase in the stress, the development of the plastic region approaches a plane stress state. That leads to increase in the characteristic dimension of the plastic zone relative to its thickness (the Dugdale model).

The Griffiths–Irwin–Orowan local-failure condition is relatively simple for the case where the maximum size of the irreversible-deformation region at the given point of the crack contour is small in comparison with the crack length and the size of the body itself. The onset of plastic deformation is observed when the tangential stress reaches the shear yield point; the culmination of the process is macroscopic disintegration. Deformation occurs as a result of slipping, twinning, and relative motion of the grains. At the atomic level, different methods of dislocational motion in the slip and twinning planes lead to intragrain shear [6]; the diffusion of point defects along the grain boundaries lead to intergrain shear. The diffusion rate of vacancies is less than the speed of the dislocations, which is comparable with the speed of sound (about 5000 m/s). Essentially, the dislocations form a boundary line between the part of the crystal characterized by shear deformation and that with no shear [7]. The lattice distortion is determined almost completely by the position of the dislocation lines and the direction of their Burgers vectors. In the general case, the dislocation line is an arbitrary spatial curve, while the Burgers vector is constant. The dislocations either form a loop or reach another surface. This surface may be the external face of the crystal or the boundary between crystallites. Since the Burgers vector is constant over the length of the dislocation line, the structure of the dislocation will change when the dislocation line rotates relative to the direction of slip. In Fig. 11, we show the geometric dimensions used in estimating the physical failure process and the corresponding stress and strain fields [4, 5].

According to Fig. 11, the models of failure may be divided in terms of their geometric dimensions, as follows:

—submicroscopic models (atomic dimensions, around 10^{-9} m), when atomic bonds are broken;

—microscopic models (around 10^{-7}–10^{-5} m), when microcracks are formed at the grain boundaries;

—macroscopic models (around 10^{-3} m), when cracks are formed and move out of the stress-concentration region.

In terms of the machining process, we may distinguish between the following processes [5]:

—plastic failure with plastic deformation over the whole volume of the body (pressure-based machining processes, such as rolling);

—brittle failure on account of crack propagation (at about 2000 m/s) with plastic deformation in a small region (cutting).

Brittle failure occurs when the stress exceeds the brittleness threshold, which depends on the phase state, chemical composition, and structure of the material, the type of crystal lattice, the temperature, and the strain rate.

Crack trajectories may be plotted by determining the angle between the initial and subsequent directions of crack growth at the tip [6]. Assuming that each small increment in the load is accompanied by small increase in the crack length, we may find the angle determining the line of increase in crack length on the basis of the failure criterion. The equation for the crack trajectory is determined from the condition of zero stress-intensity coefficient.

Thus, the development of a theory regarding the physical principles of failure provides the basis for the creation of physical cutting configurations and their use in solving practical cutting problems. In Fig. 12, we present concise data regarding the models of cutting in the order of publication. Detailed analysis of the models most commonly used, in terms of plasticity theory, may be found in [8].

On the basis of the model structures already described, we evidently need to study models at different geometric levels (by analogy with Fig. 11), since the physical processes describing the behavior of the structures and models will also be different in this case. Note that the cutting diagrams in Fig. 12, which are used to determine the main cutting characteristics and parameters, are based on elasticity and plasticity theory and models of the plane stress state in which failure and shear of the layer of material is due to the tangential stress component $\tau = (K/\sqrt{2\pi r})f_\tau(\theta)$ in Eq. (1).

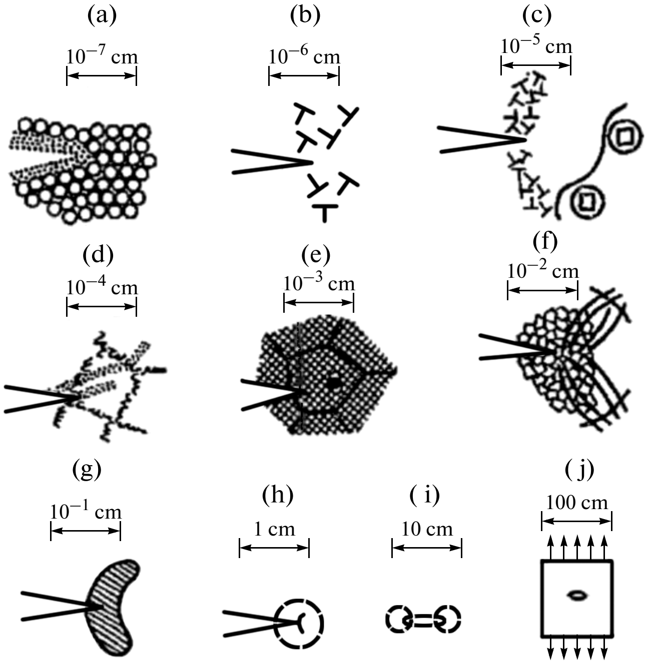

Fig. 11. Geometric relations in physical failure processes: (a) ions and electron gas; (b) dislocations; (c) boundaries of subgrains and deposits; (d) subgrains and slip bands; (e) grains, inclusions, vacancies; (f) large plastic deformation; (g) elastoplastic field with a plane deformed state; (h–j) plane stress state; (h) singular point of an elastic field; (i) transition region; (j) rated stress.

The researchers who proposed the given cutting diagrams considered cutting processes with different combinations of the magnitude, shape, and position of the crack and the plastic zone at its tip. A cutting diagram based on the plastic flow of the cut material was presented in [8]. This diagram will only be correct if the Mises plastic-flow condition is satisfied, as noted in [9]. In that case, division of the strain equations by the time permits formal conversion from strain increments to strain rates. In form, the resulting equations will resemble the equations of viscous liquid flow and hence a relation may be established between the theory of viscous liquid flow and the theory of plastic deformation. The equations of plastic flow are fundamentally different from the equations of viscous flow, since it is always possible to eliminate the time and obtain strain equations [9].

The principles used in formulating cutting diagrams, their characteristics, and the corresponding models are of great importance in identifying the structures of cutting processes, when attention focuses not on the physical phenomenon but only on the components determining the feasibility of the physical process. In considering the cutting process, its elements are position vectors and motion vectors (speed and force vectors), which in all cases ensure the required stress–strain state for the cutting process.

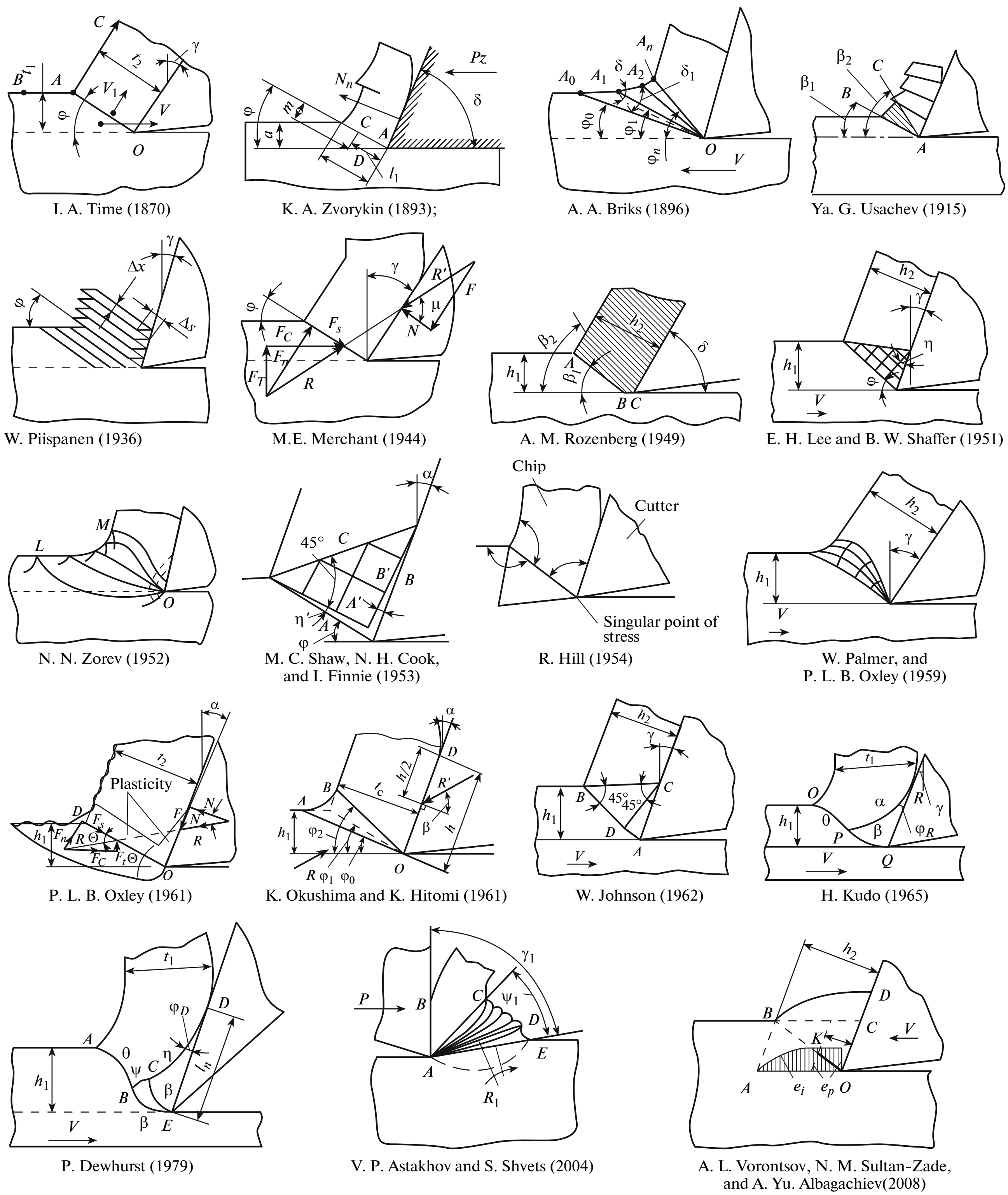

Fig. 12. Models of the cutting process in order of publication (1870–2008).

Over time, the development and applications of cutting processes will evolve. In terms of the machining of parts of different geometric dimensions, with different chip thickness, we may distinguish between submicronic cutting (around 10^{-6} m), microcutting (around 10^{-5}–10^{-6} m), fine cutting (around 10^{-4}–10^{-5} m), regular or traditional cutting (around 10^{-3}–10^{-4} m), and thick or heavy-duty cutting ($>10^{-3}$ m). Table 7 pre-

Table 7. Characteristics of nanocutting and standard cutting [10]

Characteristic	Process	
	nanocutting	standard cutting
Fundamental principles of cutting	Discrete molecular mechanics/micromechanics	Continuum mechanics/elasticity/plasticity/failure mechanics
Material of blank	Nonuniform (with microstructures)	Uniform (ideal element)
Cutting physics	Atomic cluster or microelement model: $q_i = \partial H/\partial p_i$; $p_i = -\partial H/\partial q_i$	Plane shear model (constant points in material)
	First primary stress (taking account of crystal deformation): $\sigma = \frac{1}{S}\sum_{i=1}^{N_A}\sum_{j=1}^{N_B} f_{ij} - \frac{1}{S}\sum_{i=1}^{N_A}\sum_{j=1}^{N_B} f_{0ij}$	Cauchy stress principle: $\tau_s = \frac{F_s}{A}$ (constants)
Cutting force and energy:		
type of energy	Interatomic potential functional energy: $U(r^N) = \sum_i \sum_{<i} u(r_{ij})$	Power of shear/friction: $P_s = F_s V_s$; $P_u = F_u V_c$
unit energy	High	Low
cutting force	Interatomic forces F_i: $\sum_{j \neq i}^{N} F_{ij} = \sum_{j \neq i}^{N} -\frac{du(r_{ij})}{dr_{ij}}$	Plastic deformation/friction: $F_c = F(b, d_c, \tau_s, \beta_\alpha, \varphi_c, \alpha_r)$
Chip formation:		
source of chip	Intracrystalline deformation (point defects or displacements)	Intercrystalline deformation (cavities at the grain boundaries)
strain and stress	Variable	Constant
Cutting tool:		
radius of cutting edge	Significant	Insignificant
tool wear	Rear tool surface and cutting edge	Front surface of cutting tool

sents the structure components and parameters corresponding to the commonalities and differences of standard (traditional) cutting processes and nanocutting [10].

In Fig. 13, we show a generalized structural model of the cutting process and equipment, based on the foregoing dynamic analysis of the development of physical models. This model takes account of the general characteristics used in the description and representation of those models and is formulated by means of structural models of the technological processes and the structural model F_p of the physical processes

$$F_p = L_p(V_i, P_{V_j}, t_{ij}). \quad (2)$$

Here L_p is the transformation operator for the interaction; V_i is the type of interaction; P_{V_j} are the parameters of the objects of interaction; t_{ij} is the interaction time.

In this generalized structural model of the cutting process and equipment, the interaction of type V_i corresponds to the interaction of solids with interaction parameters P_{V_j} in the form of position and motion vectors, while the transformation operator is the transformation operator L_p of the coordinate systems [1, Fig. 9]. Depending on the problem to be solved, this operator ensures the following processes.

A. Euclidean transformation of the coordinates without change in form. In other words, translation, rotation, and scale change are possible.

B. Affine transformation of the coordinates, when change in shape is permitted. In other words, translation, shear, rotation, and scale change are possible, but the basic structure cannot be changed: straight lines remain straight lines, parallel lines remain parallel, and so on.

C. Projective transformation of the coordinates permitting change in the basic structure. In other words, translation, shear, rotation, and scale change are possible, with structural modification, but straight lines remain straight lines.

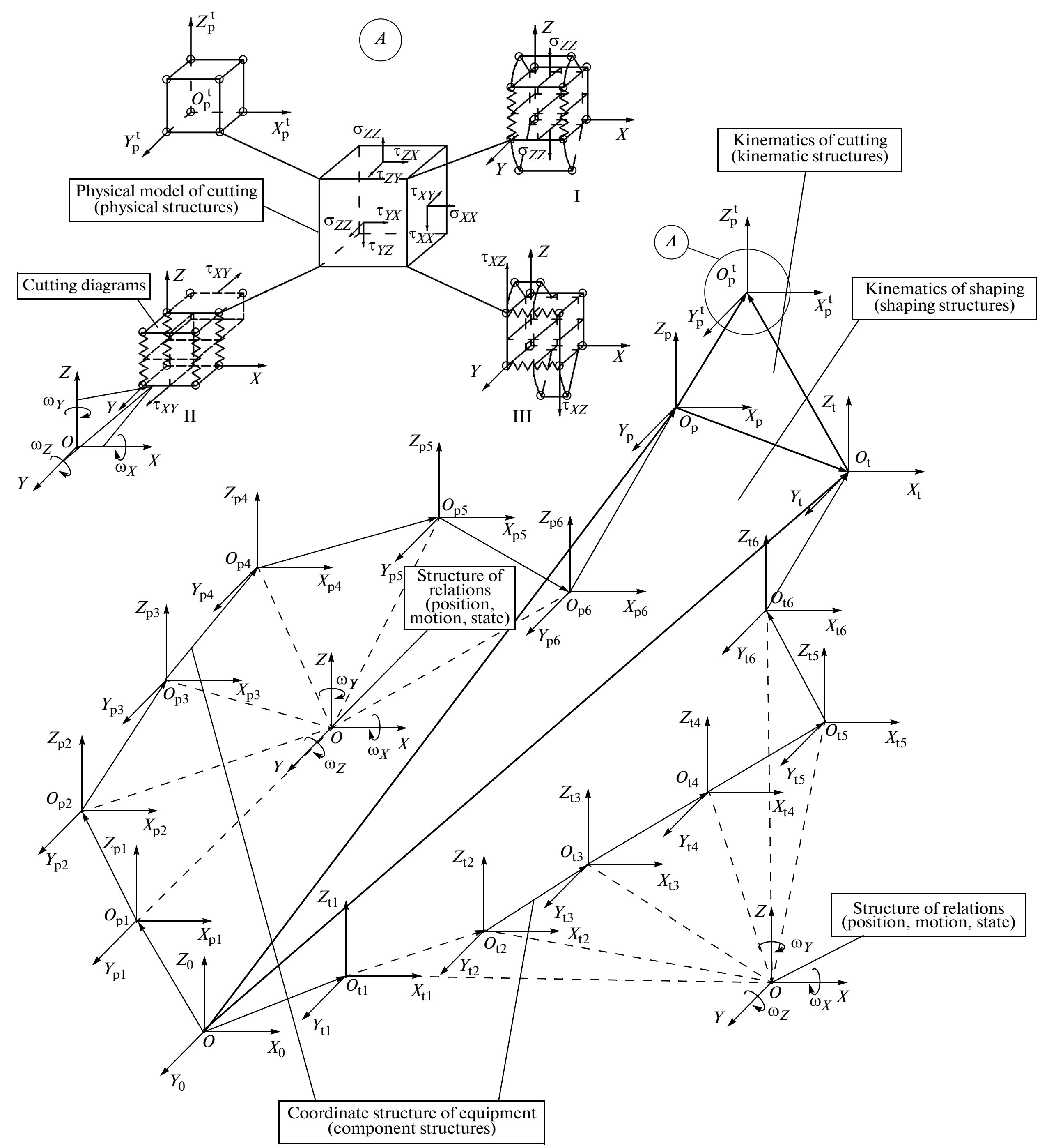

Fig. 13. Generalized structural model of the cutting process and equipment.

D. Transformation of technologies permitting change in shape. In other words, translation, shear rotation, and change in scale and shape are possible. However, points always belong to the same lines, lines to the same surfaces, and so on. In other words, the operator of each group of transformations remains invariant with respect to particular properties of the geometric figures.

Therefore, in Fig. 13, we introduce coordinate systems with centers at the points O_0; O_{t1}, …, O_{t6}; O_{p1}, …, O_{p6}; O_t; O_p^t. Here subscript 0 corresponds to the independent general coordinate system; subscripts t1, …, t6 correspond to coordinate systems associated with possible positions and motion of the tool; subscripts p1, …, p6 correspond to coordinate systems associated with possible positions and motion of the part;

and subscripts t and p correspond to coordinate systems associated with the points at which the tool and part are attached, respectively. Finally, O_p^t corresponds to the coordinate system associated with the point where the tool and part interact—that is, with the point where cutting occurs.

The constraint structure determines the mutual position and motion of the corresponding coordinate systems [11–13]. Their state determines the change in position and/or motion of the radius vectors between the centers O_i and O_{i-1} and the coordinate systems in their spatial, force, thermal, gravitational, and temporal fields. Each right-angled coordinate system permits three linear motions along the coordinate axes and three rotary motions around them. Thus, there are six motions, corresponding to the degrees of freedom of a solid body. The mutual position is also determined by six position components: three linear components in the direction of the coordinate axes and three rotary components around them. In constructing the coordinate systems of the generalized model, the OZ axis is always perpendicular to the plane of motion or the coupling plane; for a physical model of cutting, it is always perpendicular to the dislocation plane. In addition, the generalized model is constructed in the plane perpendicular to the crack's propagation front.

Thus, in Fig. 13, we show the possible number of coordinate systems, each of which is characterized only by a single degree of freedom (translation or rotation), whereas the mutual position of two coordinate systems is determined by six parameters: three linear parameters and three rotary parameters.

Then the coordinate system with center O_p^t determines the interaction of the solid bodies (the part and tool) and corresponds to the positional coordinate of the stress tensor at the crack tip in accordance with the diagram in [5, p. 24]. At pointy O_p^t, contact must also ensure equal normal and tangential contacting surfaces of the solids, velocity vectors of the part and tool, and their first and second derivatives.

We may also draw the following conclusions from Fig. 13.

1. Models I–III of failure determine the physical structure of the process. This is the physical model of cutting (the physical process of plastic deformation and disintegration).

2. The range of the module of the difference in positions of the vectors O_0O_p and O_0O_t with vertices at points O_t and O_p determine the volume of the working space.

3. The geometric and spatial relations between the positions and coordinates of the vectors $O_pO_p^t$,and $O_tO_p^t$ determine the structure of the cutting diagram (the spatial position of the model of the physical cutting process).

4. The change in mutual motion of the vectors $O_pO_p^t$, $O_tO_p^t$, and O_tO_p determines the kinematic structures (the kinematics of cutting) [14].

5. The number of motions of vectors O_0O_p and O_0O_t determines the coordinate structures (the component structure of the equipment) [11–13].

6. The change in mutual motion of the vectors O_0O_p and O_0O_t determines the shaping of the coordinate structures and hence the corresponding kinematic structures (the shaping kinematics; Table 8).

Then the transformation operator L_p may be written as follows in uniform coordinates

$$\begin{gathered} L_p\mathrm{M}_t = \mathrm{M}_p^t = \mathrm{M}_t^{po}\mathrm{M}_t^p\mathrm{M}_{6t}^{po}\mathrm{M}_{6t}^p \\ \times \ldots \times \mathrm{M}_{1t}^{po}\mathrm{M}_{1t}^p\mathrm{M}_0^{po}\mathrm{M}_{1p}^p \times \ldots \times \mathrm{M}_{6p}^{po}\mathrm{M}_{6p}^p\mathrm{M}_t. \end{gathered} \tag{3}$$

Here M_t is the matrix of the moving object (point, line, etc.); M_{it}^{po}, M_{ip}^{po} are the positional matrices of the relations between the coordinate systems

$$\mathrm{M}_{it,\,p}^{po} = \begin{vmatrix} \cos\alpha_{xx} & \cos\alpha_{xy} & \cos\alpha_{xz} & a_x \\ \cos\beta_{yx} & \cos\beta_{zy} & \cos\beta_{yz} & a_y \\ \cos\gamma_{zx} & \cos\gamma_{z\gamma} & \cos\gamma_{zz} & a_z \\ 0 & 0 & 0 & 1 \end{vmatrix}$$

and $\mathrm{M}_{it,\,p}^p$ are the motion matrices of the coordinate systems of the moving structural elements

$$\mathrm{M}_{it,\,p}^p = \begin{vmatrix} \alpha_{11} & \alpha_{12} & \alpha_{13} & l_i\cos\varepsilon_i \\ \alpha_{21} & \alpha_{22} & \alpha_{23} & l_i\cos\varphi_i \\ \alpha_{31} & \alpha_{32} & \alpha_{33} & l_i\cos\xi_i \\ 0 & 0 & 0 & 1 \end{vmatrix}.$$

In addition α_{ij} is the rotary-motion function of the coordinate system; l_i is the displacement; $l_i\cos\varepsilon_i$, $l_i\cos\varphi_i$, $l_i\cos\xi_i$ are the directional cosines of the directions of motion ($i = 1$–6).

In general, α_{ij} and l_i are functions of the time.

If we substitute α_{ij} and l_i into $\mathrm{M}_{it,\,p}^p$, we obtain the motion matrix determining the specified law of motion.

The coordinates of point O_p^t in the independent general coordinate system $OX_0Y_0Z_0$ take the form

$$\mathrm{M}_p^0 = \mathrm{M}_p^{po}\mathrm{M}_p^p\mathrm{M}_{6t}^{po}\mathrm{M}_{6p} \times \ldots \times \mathrm{M}_{1p}^{po}\mathrm{M}_{1p}^p\mathrm{M}_p;$$

$$\mathrm{M}_t^0 = \mathrm{M}_t^{po}\mathrm{M}_t^p\mathrm{M}_{6t}^{po}\mathrm{M}_{6t} \times \ldots \times \mathrm{M}_{1t}^{po}\mathrm{M}_{1t}^p\mathrm{M}_t.$$

Regardless of the selected method (the number and sequence of coordinate systems), the coordinates at point O_p^t must always be equal. In other words, we

Table 8. Shaping methods

Author	Year	Title of publication	Presentation of the method and cutting diagram	Basic principle, model	Comments;
G. I. Granovskii	1948	Cutting kinematics	Graphic display of cutting diagrams	Cutting diagrams and their classification	Combinations of one, two, three, or more from six
L. N. Koshkin	1982	Rotor and rotor–conveyor lines	Graphic display of cutting diagrams	Classification by type of part–tool interaction and their relative motion	Type of relations of the transport and cutting motions of the part and tool
E. G. Konovalov	1961	Fundamentals of new metal-working methods	Set theory, topology	The surface as the product of two topological spaces	Type of generation of the generatrix and directrix: discontinuous, continuous
A. O. Etin	1964	Kinematic analysis of methods of metal cutting	Graphic display of cutting diagrams	Cutting diagrams of surfaces of revolution, plane surfaces, and helical surfaces: turning, milling, planing	Combinations of primary and supply motions with different positions of their axes
V. S. Lyukshin	1967	Theory of helical surfaces in cutter design	Differential geometry, screw surfaces	Use of a mobile benchmark in plotting helical lines and surfaces	Method of formation of cutting tools for rolling operation
P. R. Rodin	1977	Fundamentals of the shaping of cutting surfaces	Analytical and differential geometry	Motion of the surface of the part relative to the tool, with axoids of linear, plane, annular, conical, or hyperboloid form	Shaping diagrams based on two motions of the part and tool: translation and rotation
B. A. Perepelitsa	1981	Affine-space mappings in the theory of cutting-surface shaping	Affine coordinate transformations	Matrix form of the complex motion as a combination of rotation and displacement of the benchmarks	Generation of 30 shaping diagrams
A. S. Pronikov, V. S. Satrodubov, A. P. Kuznetsov	1980, 1981	Methodological recommendations MR33–81: Reliability in engineering	Transformation of coordinate systems	Matrix form of the complex shaping motion as a combination of rotation and displacement with specified form of the cutting section	Geometric constructs of the part, individual geometric constructs, coordinate structures, structural formulas of constructs
D. Ts. Reshetov and V. T. Portman	1986	Precision of metal-cutting machines	Affine coordinate transformations	Matrix form of the complex motion as a combination of rotation and displacement, with three types of constraints	Shaping systems, shaping diagrams, diagrams of machine-tool combinations
A. I. Golembievskii	1986	Systematic analysis of shaping methods in manufacturing	Set algebra. Graphic display of shaping diagrams	Reproduction of the generatrix and directrix by slip or rolling, with continuous, discontinuous, or one-time motion	Classes of surface formation, kinematic classes of S systems and subsystems
S. P. Radzevich	2001	Surface shaping of parts: Fundamentals of the theory	Differential geometry	External and internal contact of the axoids in the form of single-pole hyperboloids of revolution	Kinematic diagrams of surface shaping of the part
Yu. M. Ermakov	2005	Hybrid methods for effective cutting	Graphic display of cutting diagrams and their classification	External and internal contact of the axoids in the form of single-pole hyperboloids of revolution	Hybrid methods in terms of the type of action, the working section, the shape, and the position of the tool; and the direction and relationships of the motion

require satisfaction of the condition $M_p^0 = M_t^0$, which ensures interaction of the solid bodies [1, Fig. 9].

If the coordinate systems are orthogonal and are not crossed, their position may be described and determined by a sequence of rotations around coordinate axes *OX*, *OY*, and *OZ*—that is, the corresponding rotation matrices. The general position matrix $M_{t,p}^{po}$ will be determined by the product of three rotation matrices, each of which describes rotation around of the coordinate axes

$$M_{i,p,t,x}^{po,p} = \begin{vmatrix} 1 & 0 & 0 & a_x \\ 0 & \cos\alpha_x & -\sin\alpha_x & a_y \\ 0 & \sin\alpha_x & \cos\alpha_x & a_z \\ 0 & 0 & 0 & 1 \end{vmatrix};$$

$$M_{i,p,t,y}^{po,p} = \begin{vmatrix} \cos\alpha_y & 0 & -\sin\alpha_y & a_x \\ 0 & 1 & 0 & a_y \\ \sin\alpha_y & 0 & \cos\alpha_y & a_z \\ 0 & 0 & 0 & 1 \end{vmatrix};$$

$$M_{i,p,t,z}^{t,p} = \begin{vmatrix} \cos\alpha_z & -\sin\alpha_y & 0 & a_x \\ \sin\alpha_z & \cos\alpha_z & 0 & a_y \\ 0 & 0 & 1 & a_z \\ 0 & 0 & 0 & 1 \end{vmatrix}.$$

If we introduce a generalized velocity coordinate and divide Eq. (3) by the time *t*, we obtain a generalized velocity structure of the model

$$\begin{aligned} \overline{M}_p^t &= M_{po}^{po}\overline{M}_t^p M_{6t}^p \overline{M}_{6t}^p \\ &\times \ldots \times M_{1t}^{po}\overline{M}_{1t}^p M_0^{po} M_{1p}^{po}\overline{M}_{1p}^p \times \ldots \times M_{6p}^{po}\overline{M}_{6p}^p \overline{M}_t, \end{aligned} \tag{4}$$

where M_t is the matrix of the moving object (point, line, etc.).

Obviously, in the limiting case, the position and motion matrices will be unit matrices. If all six position and motion matrices are unit matrices, we obtain only the coordinates of point O_p^t in the independent coordinate system $OX_0Y_0Z_0$.

Hence, the total number of structural diagrams for the cutting process is determined as the number of combinations C_n^k of *k* elements (the number of uniform position and motion matrices forming the structure of cutting) from a set of *n* (the total number of uniform position and motion matrices. Consider the example where $C_{72}^2 = 2556$; $C_{72}^3 = 59640$; $C_{72}^4 = 1028790$; $C_{72}^5 = 13991544$; $C_{72}^6 = 156238908$; $C_{36}^2 = 630$; $C_{36}^3 = 7140$; $C_{36}^4 = 58905$; $C_{36}^5 = 376992$; $C_{36}^6 = 1947792$. In that case, $n = 72$ if the uniform matrices are repeated in the position and motion structure of the part and tool and $n = 36$ if not.

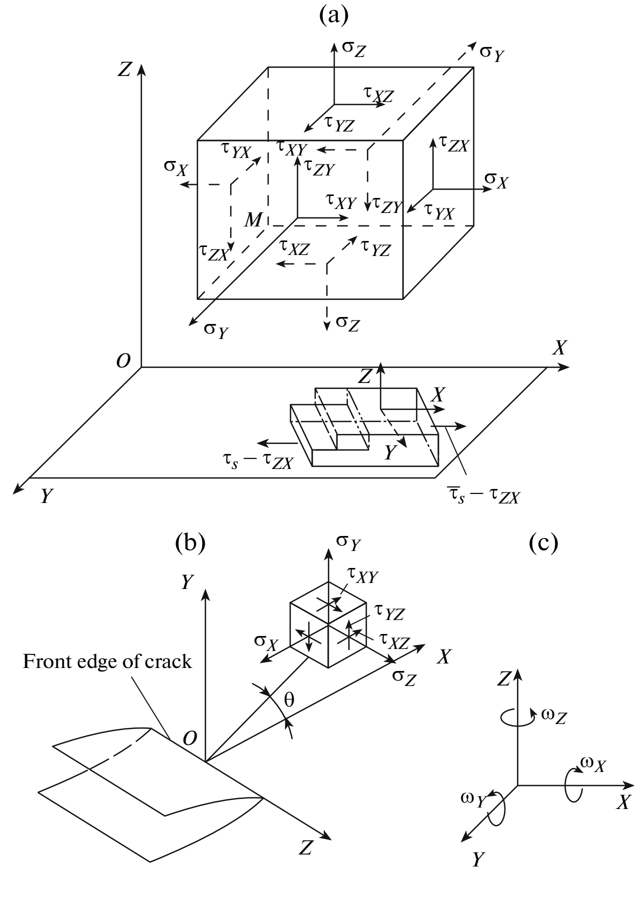

Fig. 14. Structure of the coordinate systems: (a) stress tensor of the shear dislocations; (b) front of crack; (c) position and motion matrices.

For cutting, the model of failure determines the physical structure of the process—the physical model of cutting (that is, the physical process of plastic deformation and failure). In the present case, as already noted, the model of failure is determined by the plane stress state, for different cutting diagrams in the cross section *ZOX* (Fig. 14b) [4, 5]. For shear dislocation in the *XOY* plane, the stress tensor of the plane stress state (Fig. 14a) takes the form

$$T_\sigma = \begin{pmatrix} \sigma_{XX} & 0 & \tau_{XZ} \\ 0 & 0 & 0 \\ -\tau_{ZX} & 0 & \sigma_{ZZ} \end{pmatrix}.$$

The cutting diagram and structural model for shear dislocations in the *ZOY* and *ZOX* planes will be analogous. Therefore, in what follows, we only consider the shear model and structural models in the *XOY* plane. The results will also correspond to the stress state in the other planes. By analogy with the shear-stress tensor $\bar{\tau}_s = \tau_{ZX}$, the velocity $\bar{v}_s = v_{ZX}$ (velocity tensor) and its components take the form

$$v_{ZX}(\tau_{ZX}) = v_{ZX} + v_{YX} + R\omega_Y = v_{YX} + v_{ZX} + R_{ZO}\omega^z_{YO} + R_{YO}\omega^y_{YO} + R_{XO}\omega^x_{YO}.$$

Here v_{ZX} and v_{YX} are the linear velocity vectors of the axes *ZO* and *YO*, respectively, along the *XO* axis in the shear plane *XOY*; $R\omega_Y$ is the linear velocity vector for the rotation of radius vector R relative to the *YO* axis in the shear plane *XOY*; $R_{ZO}\omega^z_{YO}$ is the linear vector for the rotary velocity ω^z_{YO} of the *YO* axis at a distance R_{ZO} from shear plane *XOY*; $R_{XO}\omega^x_{YO}$ is the linear vector for the rotary velocity ω^z_{YO} of the *YO* axis at a distance R_{OX} in the shear plane *XOY* relative to the *YO* axis; $R_{YO}\omega^y_{YO}$ is the linear vector for the rotary velocity ω^y_{YO} relative to the *YO* axis of radius vector R_{OY} at the *YO* axis of the shear plane.

The tangential stress τ_s determining the dislocational shear is $\tau_s = \tau_{XZ} = F_s/S_s$, where F_s is the dislocational shear force; S_s is the area on which the tangential stress acts. Shear occurs with equal tangential stress and forces exerted by the part and the tool. (The frictional force is disregarded here.) As a result, we obtain

$$\bar{F}_s = \bar{\tau}_s S_s = m_s a_s = \rho V_s \bar{v}_s / t_s = \sum \bar{F}_{\mathrm{tp}} = m_{\mathrm{p}} a_{\mathrm{p}} + m_{\mathrm{t}} a_{\mathrm{t}} = m_{\mathrm{p}} \bar{v}_{\mathrm{p}}/t + m_{\mathrm{t}} \bar{v}_{\mathrm{t}}/t,$$

where a_s and $\bar{v}_s$ are the acceleration and velocity vector of the dislocation; t_s is the time of dislocational motion; V_s is the volume of the displaced dislocation; m_{p} is the mass of the part; m_{t} is the mass of the tool; $\bar{v}_{\mathrm{p}}$ is the velocity vector of the part; $\bar{v}_{\mathrm{t}}$ is the velocity vector of the tool; t is the cutting time.

More precise values of the cutting forces were presented by the authors mentioned in Fig. 12. In the present case, the structure of the cutting force is important. We may write $\bar{F}_s = \bar{\tau}_s K_s$, where K_s is determined by the relevant cutting model (Fig. 12) and depends on the type and number of parameters taken into account (the linear and angular dimensions, physical properties, type of friction, etc.) and their degree of detail. At the same time, the work of the cutting force is determined by the cutting force and cutting speed and hence by the cutting structure in accordance with Fig. 13. We may determine the structural components of the cutting speed and then, on the basis of Eq. (4), write the kinematic equation for the velocity at point $O^{\mathrm{t}}_{\mathrm{p}}$

$$\bar{v}^{\mathrm{t}}_{\mathrm{p}} = \bar{v}^{O_{\mathrm{p}}}_{O} - \bar{v}^{O_{\mathrm{t}}}_{O} + \bar{v}^{O^{\mathrm{t}}_{\mathrm{p}}}_{O_{\mathrm{p}}} - \bar{v}^{O^{\mathrm{t}}_{\mathrm{p}}}_{O_{\mathrm{t}}},$$

here $\bar{v}^{O_{\mathrm{p,t}}}_{O}$, $\bar{v}^{O^{\mathrm{t}}_{\mathrm{p}}}_{O_{\mathrm{p,t}}} = \bar{v} + \omega r$; $\bar{v}^{O_{\mathrm{p}}}_{O}$, $\bar{v}^{O_{\mathrm{t}}}_{O}$ are the velocity vectors at the points of attachment of the part (O_{p}) and tool (O_{t}); $\bar{v}^{O^{\mathrm{t}}_{\mathrm{p}}}_{O_{\mathrm{p}}}$ $\bar{v}^{O^{\mathrm{t}}_{\mathrm{p}}}_{O_{\mathrm{t}}}$ are the velocity vectors at the point $O^{\mathrm{t}}_{\mathrm{p}}$ of part–tool contact.

Obviously, the vector sums of the velocities are determined by the cutting methods, characterized by their relationship. The cutting kinematics is determined by the position and motion vectors according to the structure of the transformation operator L_p in the uniform coordinates in Eq. (2), whereby the type of cutting methods of the same kinematic structure will be different. Thus, the relation between three cutting speeds was considered in [15]: the turning speed (with rotation of the part); the planing speed (with linear motion of the tool or part); and the milling speed (tool rotation). The general characteristics of the cutting kinematics and the types of machining methods for identical kinematic structures were shown. In addition, proposals for the design of hybrid methods on that basis were made.

In the present work, we do not investigate the relations obtained on the basis of structural constraints. Instead, we present elements of the cutting process as systems and determine the constraints and relationships forming the structure of the system. Then the geometric and spatial relations of the mutual positions and the characteristic coordinate values of the vectors $O_{\mathrm{p}}O^{\mathrm{t}}_{\mathrm{p}}$ and $O_{\mathrm{t}}O^{\mathrm{t}}_{\mathrm{p}}$ determine the structures of the cutting diagrams (the spatial position of the model of the physical cutting process), as shown in Fig. 15. The structures of the cutting diagrams in Table 9 are obtained on the basis of the physical model of cutting (Figs. 10, 13, and 14) as longitudinal plane shear of the dislocations by the cutting tool. Note that the structure in Fig. 15a corresponds to model II (Figs. 10 and 14), where, instead of the tangential stress, the cutter resulting in shear and separation of part of the material from the part in the plane is shown. The characteristic adopted here is zero curvature of the tool (ρ_{t}) and part (ρ_{p}). This corresponds to infinite radii of the part (R_{p}) and tool (R_{t}) at the con-

Table 9. Construction of possible kinematic structures for cutting

Configuration				Tool					
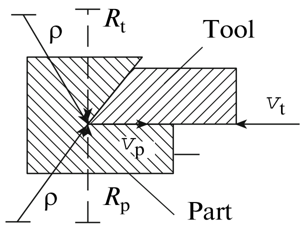				$\rho_p = \rho_t$	$\rho_p > \rho_t$	$\rho_p < \rho_t$	cutting motion	shaping motion or position	$v_p^t = v_t/v_p$
				$\rho > 0$	$\rho < 0$	$\rho = 0$			
				mobile	mobile	immobile			
				→	←	/////			
Part	$\rho < 0$	Mobile	↓	v_t → ← v_p	v_t ← ← v_p	v_p →	Linear	Motion 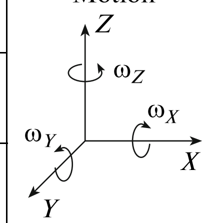	$v_p^t = 0$; $0 < v_p^t < 1$; $v_p^t > 1$; $v_p^t \longrightarrow \infty$
						/////	Rotary		
	$\rho > 0$	Mobile	↑	v_t → → v_p	v_t → ← v_p	v_p →	Linear		
						/////	Rotary	Position 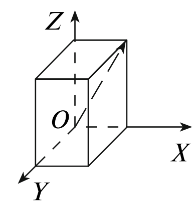	
	$\rho = 0$	Immobile	/////	v_t →	v_t ←	/////	Linear		
				/////	/////	/////	Rotary		

Type of motion	Linear	Rotary	Linear	Rotary	Linear	Rotary	Region of force, thermal, temporal, and other fields
Shaping motion or position	Motion 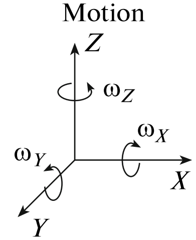			Position 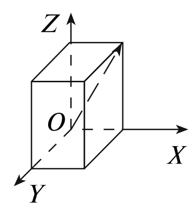			
$v_p^t = v_t/v_p$	$v_p^t = 0$; $0 < v_p^t < 1$; $v_p^t > 1$; $v_p^t \longrightarrow \infty$						

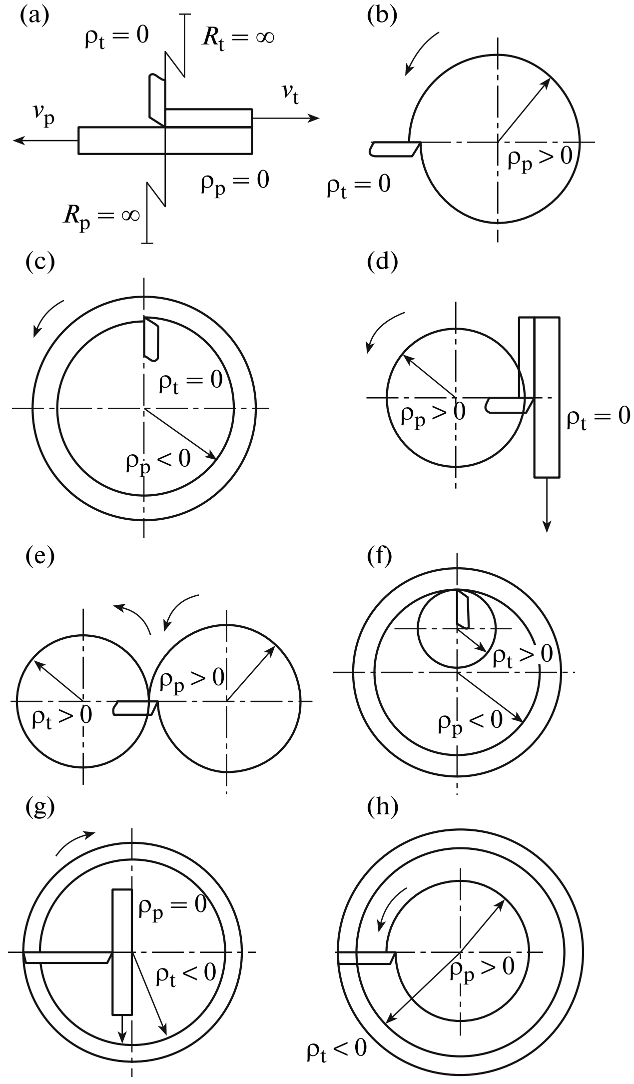

Fig. 15. Structure of the cutting diagrams.

tact point. To obtain the structures in Figs. 15a–15d, the curvature (radius) of the part is modified with constant curvature of the tool. In other words, physical model II is retained. In Figs. 15e and 15f, positive tool curvature is maintained ($\rho_t > 0$), whereas, in Figs. 15g and 15h, negative tool curvature is maintained ($\rho_t < 0$), with variation in the curvature of the part from zero to positive and negative values, respectively. All the diagrams are presented in the cross section perpendicular to the front of the crack, while the shear plane is the *XOY* plane. For the *ZOX* and *ZOY* planes or planes with an arbitrary position in space, the structure of the cutting diagram is analogous.

Variation in the mutual motion of the vectors $O_pO_p^t$, $O_tO_p^t$, and O_tO_p determine the kinematic structures (cutting kinematics), which creates the final shape of the parts' surface [15]. Table 8 provides information regarding Russian research devoted to the cutting kinematics and shaping methods.

Thus, the general classification of kinematic structures for cutting (Table 9) may be based on the use of transformation operator L_p in uniform coordinates to generate a structural model (Fig. 13) of cutting in accordance with the classification system in [1, Table 5] and the proposed procedure for deriving structural components. The resulting region of states characterizes the perturbations that change the properties of the structural elements and hence change the properties of the final part–tool interaction [1, Fig. 9]. Consequently, a different machining method may be formulated for the specified kinematics. In other words, the number of machining methods for the given physical model of cutting, whose structure is described in terms of uniform coordinates, will depend on all the components of the process's technological construct, described in the form

$$T(7) = [F_f(123456), P_k(123456), P_v(123456)]$$
$$= [F_f(134678), P_k(15253645), P_v(162636)],$$

The number of possible designs is relatively large and not always obvious.

The creation of new machining methods calls for special analysis of the machining structures obtained.

REFERENCES

1. Kuznetsov, A.P., Structure of cutting processes and equipment. Part 2. Structure and classification of technological processes, *Russ. Eng. Res.*, 2015, vol. 35, no. 6.
2. Merchant, E. and Moehring, S., *An Interpretive Review of Twentieth-Century US Machining and Grinding Research*, Cincinnati: TechSolve, 2003.
3. Malyshev, V.I., *Ocherki istorii nauki o rezanii materialov* (Outlines of the History of Cutting Science), Tolyatti: TGU, 2011.
4. Parton, V.Z., *Mekhanika razrusheniya: Ot teorii k praktike* (Failure Mechanics: From Theory to Practice), Moscow: Nauka, 1990.
5. Parton, V.Z. and Morozov, E.M., *Mekhanika uprugoplasticheskogo razrusheniya* (Elastoplastic Failure Mechanics), Moscow: Nauka, 1985.
6. Bogatov, A.A., *Mekhanicheskie svoistva i modeli razrusheniya metallov* (Mechanical Properties and Failure Models for Metals), Yekaterinburg: GOU VPO UGTU–UPI, 2002.
7. Starkov, V.K., *Fizika i optimizatsiya rezaniya materialov* (Physics and Optimization of Cutting), Moscow: Mashinostroenie, 2009.
8. Sultan-Zade, N.M., Albagachiev, A.Yu., and Vorontsov, A.L., *Teoreticheskie osnovy obrabotki met-*

allov v mashinostroenii (Theoretical Principles of Metalworking in Manufacturing), Staryi Oskol: TNT, 2013.

9. Kachanov, L.M., *Osnovy teorii plastichnosti* (Fundamentals of Plasticity Theory), Moscow: Nauka, 1969.
10. *Machining with Nanomaterials*, Jackson, M.J. and Morrell, J.S., Eds., New York: Springer, 2009.
11. Kuznetsov, A.P. and Kosov, M.G., Structural precision of metal-cutting machines, *Russ. Eng. Res.*, 2012, vol. 32, no. 11/12, pp. 725–729.
12. Kuznetsov, A.P. and Kosov, M.G., Structural precision of metal-cutting machines, *Russ. Eng. Res.*, 2012, vol. 32, no. 5/6, pp. 482–490.
13. Kuznetsov, A.P., *Teplovoe povedenie i tochnost' metallorezhushchikh stankov* (Thermal Behavior and Precision of Metal-Cutting Machines), Moscow: Yanus-K, 2011.
14. Granovskii, G.I., *Kinematika rezaniya* (Cutting Kinematics), Moscow: Mashgiz, 1948.
15. Ermakov, Yu.M., *Kompleksnye sposoby effektivnoi obrabotki rezaniem* (Effective Hybrid Cutting Methods), Moscow: Mashinostroenie, 2005.

Translated by Bernard Gilbert